Tools and Technology

Evaluating Unmanned Aerial Systems for the Detection and Monitoring of Moose in Northeastern Minnesota

MICHAEL C. MCMAHON (iD),[1] *Department of Fisheries, Wildlife, and Conservation Biology, University of Minnesota, 2003 Upper Buford Circle, Suite 135, Saint Paul, MN 55108, USA*

MARK A. DITMER (iD), *Department of Fisheries, Wildlife, and Conservation Biology, University of Minnesota, 2003 Upper Buford Circle, Suite 135, Saint Paul, MN 55108, USA*

EDMUND J. ISAAC, *Grand Portage Biology and Environment, 27 Store Road, Grand Portage Band of Lake Superior Chippewa, Grand Portage, MN 55605, USA*

SETH A. MOORE, *Grand Portage Biology and Environment, 27 Store Road, Grand Portage Band of Lake Superior Chippewa, Grand Portage, MN 55605, USA*

JAMES D. FORESTER (iD), *Department of Fisheries, Wildlife, and Conservation Biology, University of Minnesota, 2003 Upper Buford Circle, Suite 135, Saint Paul, MN 55108, USA*

ABSTRACT The use of unmanned aerial systems (UAS) for wildlife surveying and research has widely expanded in the past decade, but with varying levels of success. Applying UAS paired with Forward Looking Infrared (FLIR) technology to survey forest-dwelling species has been particularly challenging because of unreliable animal detection. We describe our application of UAS and FLIR technology to detect GPS-collared moose (*Alces alces*) and their calves in the heavily-forested region of northeastern Minnesota, USA, during 2018 and 2019. We conducted grid-pattern UAS thermal surveys over GPS-collared cows during the calving seasons (April to June) of 2018 and 2019 to determine the feasibility of using a FLIR-equipped UAS for detecting cow moose, and for quantifying the number of calves. We also collected data on environmental and flight characteristic variables to model moose detection. Our best fitting model of moose detection showed increased detection with more cloud cover at the survey site ($\hat{\beta} = 1.13$, SE = 0.43), whereas increased forest canopy ($\hat{\beta} = -1.10$, SE = 0.38), and vegetative greenness (enhanced vegetation index, EVI; $\hat{\beta} = -1.37$, SE = 0.32) both reduced detection success. By adjusting our methodology based on our detection model findings, we increased our adult moose detection success from 25% during our first season, to 85% during our second season, and calf detection from 27% to 79%, respectively. We report on our methodological improvements and identify limitations to UAS-based wildlife research in forested systems. Overall, we found that UAS with FLIR sensing is a promising tool for quantifying moose calving success, twinning rate, and calf survival, and may be effective for monitoring the reproductive success and survival of other wildlife species in densely forested regions. © 2021 The Wildlife Society.

KEY WORDS aerial survey, *Alces alces*, calf survival, detection modeling, drones, FLIR, Minnesota, thermal infrared, unmanned aerial systems (UAS), unmanned aerial vehicles (UAV).

The use of unmanned aerial systems (UAS) in wildlife science has grown rapidly (Jiménez López and Mulero-Pázmány 2019) for their applications in animal surveying and censuses (Vermeulen et al. 2013, Chrétien et al. 2015, Ezat et al. 2018), detection of animal sign (e.g., nests and tracks; Goebel et al. 2015, van Andel et al. 2015), and habitat evaluation (Chen et al. 2017, Olsoy et al. 2018). Studies deploying UAS have covered a range of taxonomic groups including terrestrial and aquatic mammals (Hodgson et al. 2013, Witczuk et al. 2018), birds (Chabot and Bird 2012), reptiles (Ezat et al. 2018), and fish (Kiszka et al. 2016). Unmanned aerial systems can collect data at fine spatial and temporal resolutions because they can fly at low altitudes and much slower flight speeds relative to conventional manned aircraft (Anderson and Gaston 2013). Operational efficiency of UAS is increased with the ability to launch UAS rapidly on site with user discretion, whereas conventional aircraft often are limited by low cloud cover, require additional flight time to travel to and from refueling sites, and have a considerably higher operating cost (Chabot 2009, Watts et al. 2010, Vermeulen et al. 2013,

Linchant et al. 2015). Safety is also increased with UAS because they eliminate the need for manned-flight in often hazardous environments (Jones et al. 2006, Watts et al. 2010); low-level flight is a leading cause of job-related mortality for wildlife professionals (Sasse 2003).

Evidence suggests that the presence of UAS can disturb wildlife by eliciting behavioral (Bennitt et al. 2019) and physiological responses (Ditmer et al. 2015). However, UAS reduces the need to approach animals on foot or with ground vehicles for counting or conducting observations, and may ultimately cause less disturbance than traditional aerial counting methods with manned aircraft (Chabot and Bird 2012, Goebel et al. 2015, Weissensteiner et al. 2015, Hodgson et al. 2018) due to less noise from electric UAS motors (Mulero-Pázmány et al. 2017). Consequently, UAS provide a powerful tool for monitoring of populations where repeat visits are required to monitor parameters like nesting success or survival rates (Sardá-Palomera et al. 2012); this is especially valuable when monitoring species that are sensitive to anthropogenic disturbances (Ditmer et al. 2019).

Unmanned aerial systems can be equipped with a large variety of sophisticated sensors, and the use of multiple combinations of sensors are possible with adequate UAS payload capacity. The proliferation of UAS and sensors in a variety of scientific fields and industries has led to reduced sensor and UAS costs and improvements in the spatial resolution of sensors. Color (RGB) cameras are commonly included on UAS and yield high-resolution imagery of ground features and even wildlife (Chabot and Bird 2012; Hodgson et al. 2013, 2018). Forward Looking Infrared (FLIR) sensors are increasingly being deployed in UAS systems to successfully detect and survey homeothermic wildlife species (Witczuk et al. 2018, Ireland et al. 2019). By capturing thermal radiation emitted from animals, FLIR sensors allow for increased detection probability of species that are well camouflaged, partially obscured by vegetation, or at greater distances than could be detected with conventional methods (Dunn et al. 2002, Haroldson et al. 2003, Montague et al. 2017). These advantages reduce perception bias (i.e., failing to detect an animal that was present and available for detection; Marsh and Sinclair 1989) and have provided significant increases in the efficacy of some wildlife surveys (Focardi et al. 2001). Thermal sensing works best when there is high contrast between an animal's temperature and the background environment (i.e., a warm-bodied animal against cool ground; Garner et al. 1995, Chrétien et al. 2016). Rocks, bare ground, logs, and living trees absorb and emit large amounts of thermal radiation, which results in bright returns that can create false-positive detections (Garner et al. 1995, Dunn et al. 2002). Importantly, environments with thick vegetation or dense forest canopy can obscure wildlife from detection thus limiting the effectiveness of UAS-FLIR pairing (Gill et al. 1997, Dunn et al. 2002, Kissell and Nimmo 2011). Thermal sensors have been useful for detecting moose (*Alces alces*) and other ungulates from manned aircraft (Addison 1972, Adams et al. 1997, Bontaites et al. 2000,

Bernatas and Nelson 2004, Millette et al. 2014); similar levels of success have been achieved when affixing FLIR sensors to UAS (Chrétien et al. 2016, Witczuk et al. 2018, Ireland et al. 2019, Beaver et al. 2020), even with smaller bodied target species, such as recently born roe deer (*Capreolus capreolus*) fawns in grass meadows (Israel 2011).

Most studies to date have paired UAS with FLIR technology for wildlife detection in open terrain without a high percentage of forest cover (Israel 2011, Lhoest et al. 2015, Ireland et al. 2019). Indeed, both manned aircraft and UAS surveys using FLIR sensing in forested environments have faced greater challenges due to unreliable animal detection (Potvin and Breton 2005; Chrétien et al. 2015, 2016; Witczuk et al. 2018). Surprisingly, this was true even for large-bodied animals; Dunn et al. (2002) found that aerial FLIR sensing did not aid in detection of elk (*Cervus elaphus*) because: 1) elk were well-insulated and did not have high enough contrast in thermal imagery, 2) emitted thermal radiation from trees and bare ground confounded detection, and 3) heavy tree cover (e.g., dense coniferous forest habitat) physically obscured elk from detection. Further understanding and overcoming these limitations of FLIR-equipped UAS is critical for realizing the full potential of this technology for management and conservation applications.

Moose inhabiting northeastern Minnesota's Grand Portage Indian Reservation, USA, are an important subsistence species used by the Grand Portage Band of Lake Superior Chippewa historically and presently, but harvests have declined in recent years concomitant with significant (~65%) declines in moose populations throughout their range in Minnesota over the last decade (S. A. Moore, Grand Portage Trust Lands, unpublished data; Del Giudice 2018). This has resulted in extensive research and management efforts by the Grand Portage Band of Lake Superior Chippewa and the Minnesota Department of Natural Resources (MNDNR) to understand the drivers of the decline (Severud et al. 2015). Mortality of adult moose in MN has been linked to disease (Wünschmann et al. 2015), increased parasite loads (Verma et al. 2016), and predation (Carstensen et al. 2017). Warming temperatures and decreasing snow depth associated with climate change are also thought to be contributing to their decline by increasing thermal stress (Street et al. 2016) and allowing for the increase of white-tailed deer (*Odocoileus virginianus*) population densities (Weiskopf et al. 2019). Deer pose a threat to moose as they are known to carry transmissible diseases and parasites (Wünschmann et al. 2015). Neonate (i.e., moose calf) birthing, survival, and predation rates are critical for understanding the future population trajectory of moose (Severud et al. 2015, 2019), thus, the Grand Portage Trust Lands Department initiated an intensive study of the northeastern moose population beginning in 2008. Tribal biologists conduct annual aerial counts to monitor population demographics and have fitted moose with GPS collars to examine survival and causes of mortality. These efforts have been undertaken to conserve moose on the landscape and preserve a cultural icon for future generations.

These demographic estimates became more challenging to quantify outside of the reservation after the state of Minnesota banned moose collaring due to initially high capture-induced abandonment rates during studies of calf survival and predation (Del Giudice et al. 2015, 2018). Forward Looking Infrared-equipped UAS may provide a much needed, non-invasive tool to better estimate and track these important demographic rates of moose calves.

In this study we attempted to determine the feasibility of using UAS technology to detect cow moose and quantify the presence of any neonates while minimizing disturbance of cow-calf pairs. Our study aimed to quantify the number of calves born per cow and determine the length of calf survivorship through repeated UAS flights. We also explicitly attempted to determine what factors limited the effectiveness of UAS operations with FLIR technology to detect moose in a heavily forested environment by modeling the detection probability of adult moose during our 92 spring flight missions based on weather conditions, habitat type

and structure, UAS flight characteristics (e.g., flight altitude), and the phenology of vegetation. Our research details how wildlife researchers and managers can more efficiently utilize UAS and FLIR technologies to collect data on large ungulates in northern forested environments.

STUDY AREA

All UAS flights were conducted within the Grand Portage Band of Lake Superior Chippewa Indian Reservation and eastern extents of the Grand Portage State Forest, Minnesota, USA (Fig. 1). Topography was highly varied and ranged from 183 m to 553 m above sea level. Mean monthly temperatures for Grand Portage ranged between 1.89° C to 14.0° C during our study periods (May to June, 2018 and April to May, 2019). The mean minimum temperatures ranged between −2.94° C to 7.94° C, and mean maximum temperatures were between 6.67° C to 20.11° C. Monthly precipitation ranged from 3.86 cm to 11.28 cm
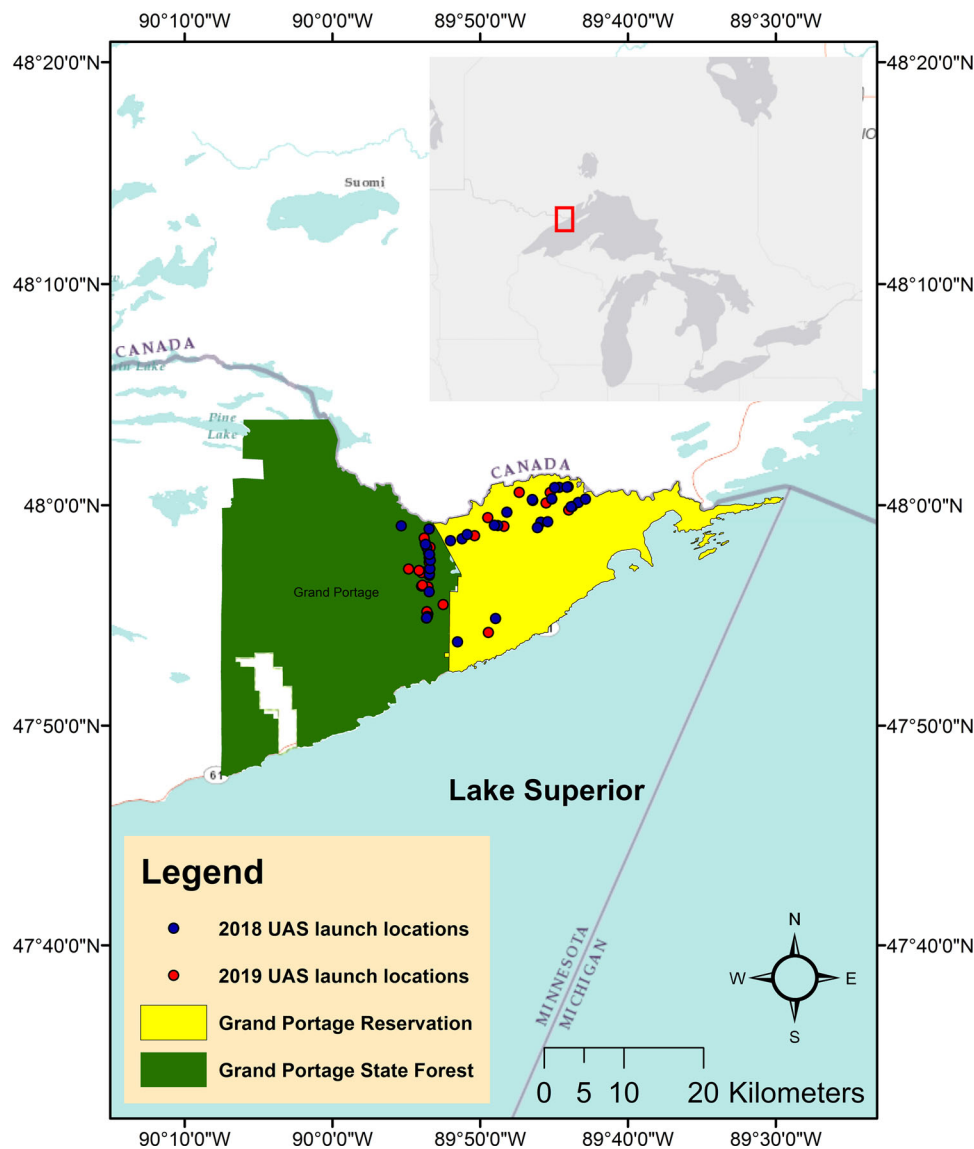
Figure 1. Study area of Grand Portage Reservation and eastern Grand Portage State Forest, in northeastern Minnesota, USA. Unmanned aerial system (UAS) launches are shown across the study area for the 2018 and 2019 field seasons.

with a mean monthly precipitation level of 6.67 cm (NOAA 2019). Snow depth during our study period ranged from 0 cm to ~60 cm (M. C. McMahon, University of Minnesota, personal observation).

Vegetation on the reservation consisted of boreal forest with aspen-birch (55%; *Populus tremuloides* and *Betula papyrifera*), conifer (25%; *Pinus strobus, P. resinosa, P. banksiana, Abies balsamea,* and *Thuja occidentalis*), northern hardwood (6%; *Acer saccharum* and *A. rubrum*), swamp hardwood (3%; *Fraxinus spp.*), and other (11%) communities (E. Isaac, Grand Portage Trust Lands, unpublished data). In addition to moose, white-tailed deer, black bears (*Ursus americanus*), and gray wolves (*Canis lupus*) were present in our study area.

METHODS

Data Collection
Our study population consisted of 22 cow moose fitted with GPS-collars with Iridium-satellite relay capabilities (VECTRONIC Aerospace, Berlin, Germany). Capture and handling of moose was conducted by the Grand Portage Natural Resources Management Department (IACUC Protocol# 1812-36635A). Moose locations were recorded and stored every 30 minutes to GPS collars, with GPS coordinates transmitted to satellites every two hours. Adult moose movement patterns can indicate a variety of critical information such as calving and either successful or attempted predation events (Severud et al. 2015, Obermoller et al. 2019). We analyzed cow moose movements multiple times a day to identify locations and times for safe and efficient UAS deployment to detect cow moose and calves. Prior to conducting flight missions above cow-calf pairs, we conducted initial test flights over GPS-collared bull moose in May of 2018 to gauge levels of disturbance from UAS flights. We would classify a disturbance if there were any erratic movements (i.e., fleeing from an area) that corresponded in time to UAS launch and flight times. Although none of these initial flights led to a behavioral disturbance, we took precautions in our surveys of cow moose and calves to reduce the risk of disturbance (see below), and continued monitoring movement behavior to identify potential disturbance responses (Hodgson and Koh 2016).

We used a DJI Inspire 2 quadcopter (~$3,000 USD; Shenzhen DJI Sciences and Technologies Ltd., Nanshan District, Shenzhen, China), equipped with a FLIR Vue Pro 640 (640 × 512 pixels, 32° FOV, 19 mm, 30 Hz) (~$3700 USD; FLIR Systems Inc., Wilsonville, OR, USA) for 2018 surveys and a FLIR Duo® Pro R (640 × 512 pixels, 32° FOV, 19 mm, 30 Hz; ~$6350 USD) for 2019 surveys. Both thermal sensors were one-band sensors with a spectral interval that measured 7.5 to 13.5 μm. The FLIR Duo® Pro R used in 2019 also featured an RGB sensor (4000 × 3000 pixels, 56° × 45° FOV) that allowed us to capture color imagery simultaneously with thermal imagery. Survey flights were planned and conducted using the Pix4Dcapture app (Pix4D, Prilly, Switzerland). Thermal infrared and RGB footage were recorded and stored onboard the UAS for review post flight.

Flights occurred from 25 May 2018 to 28 June 2018 (n = 44 flights) and 25 April 2019 to 30 May 2019 (n = 48 flights) at varying times between morning and evening civil twilight. Surveys were flown in rectangular grid transects centered over the most recently updated GPS locations of cows. Rectangular grids were used to maximize our coverage in the event that the cow moved off of the last known location prior to launching the UAS, and to minimize the risk of animal disturbance (Mulero-Pázmány et al. 2017). To minimize animal disturbance from our presence on the ground, we launched the UAS from reservation and county roads or trails that were between 300 m and 600 m Euclidean ground distance from updated moose locations. This distance also allowed us to maintain visual contact of the UAS, and sufficient radio communication between the remote and quadcopter. Additionally, we flew at altitudes that were near the maximum allowable 122 m (~400 ft) above ground level; altitudes ranged from 75 m to 121 m depending on terrain elevations relative to launch points.

Moose Demographic Data and Predation Events
Thermal infrared video footage was reviewed manually post flight by human observers. Observers were trained to detect living animals in thermal video by viewing sample footage collected over domestic animals (e.g., domestic bison, cows, and captive deer) of known location and abundance, to develop a sight picture for large-bodied mammals in thermal imagery. The same observers reviewed thermal video footage for both seasons. Adult moose and calves were visually identified from the video footage by their shape and brightness in the footage, the latter also by their proximity with the cow. Detections of target moose (i.e., bright white silhouettes that often resembled a large animal body with a head) were confirmed by updated cow GPS locations collected during and post UAS survey times. We attempted to utilize object-based image analysis (OBIA) to quantify moose detections from our thermal video footage. However, we would have needed to greatly increase the resolution of our FLIR sensors (at an economic expense), or fly the UAS at lower altitudes, increasing the risk of disturbing moose and striking hazards (e.g., tall trees), to effectively apply OBIA methods to discern moose from other objects.

For 2018 flights, moose detections were verified by matching the position of the UAS on the flight transect where a thermal detection was observed (based on flight time) to the location and time stamp from the collared moose that corresponded to that time in the flight. In 2019, detections were verified by matching GPS coordinates of the UAS and of the moose at given flight times. This was possible because the FLIR Duo® Pro R used in 2019 featured geotagged video footage that provided GPS coordinates for the UAS every second of survey time, whereas the FLIR Vue Pro used in 2018 did not. Color (RGB) footage was also reviewed for flights with positive thermal detections as an additional verification throughout the 2019 season. Thermal detections of cows and counts of calves were recorded for each flight.

We investigated suspected calf predation events by flying over known collared cow-calf pairs after large movements occurred in a short period of time, with the cow commonly circling back to the suspected predation location. We considered a predation event to be positively confirmed if we could detect the cow without the previously detected calf. Conversely, we concluded that a predation event was unsuccessful or did not occur by thermally detecting the calf with its mother. Our conclusions about predation events through remote sensing were corroborated by subsequent on-foot investigations.

Moose Detection Variables

To better understand what factors altered our ability to detect moose using UAS with FLIR technology, we developed a detection model that included data on weather conditions, UAS operations, habitat type, and vegetation structure and phenology. Factors that we hypothesized would influence detection included: 1) cloud cover, which was recorded in the field from visual observations; 2) temperature; 3) relative humidity; 4) wind speed; 5) mean altitude; 6) canopy cover; 7) forest composition; and 8) vegetation phenology. Temperature, humidity, and wind speed were collected post flight with archived weather data recorded at the Cook Municipal airport (Cook, MN, USA; 47.82°N, −92.69°W; National Oceanic and Atmospheric Administration 2019). We recorded altitude of the UAS throughout each flight and summarized these data as mean altitude for our detection models. Light Detection and Ranging (LiDAR) was collected throughout the region during May 2011 (a leaf-free period in the study area) at a rate of 1 pulse/meter with a vertical accuracy RMSE of 5.0 cm and a horizontal accuracy of 1.16 m (Minnesota Geospatial Information Office 2018). We estimated percent forest canopy as the percentage of LiDAR returns that were >3 m above the ground, based on subtracting the return values from a Digital Elevation Model (DEM) with a spatial resolution of 3 m, within a 30-m resolution grid that covered the study area. We assigned each flight a canopy cover percentage based on the maximum canopy cover value within 20 m of the moose's GPS-location during the UAS flight (see rationale in the Moose Detection Modeling

section). Because we believed conifer cover would reduce moose detection, even in early spring, we included the total percentage of conifer and mixed conifer-deciduous forest within the same buffer. Land cover was derived from a multitemporal composite of Landsat 8 imagery combined with LiDAR data (Minnesota Geospatial Information Office 2016). To estimate the phenology on a given day at a particular UAS flight area, we used the enhanced vegetation index (EVI) from the MODIS data set collected by the National Aeronautics and Space Administration (NASA). The MODIS dataset provides remotely sensed estimates of vegetative greenness at a 500-m spatial resolution composited over a 16-day period (MODIS/Terra Vegetation Indices 16-day L3 Global 500-m resolution, MOD13A1; Didan 2015); we used the MODIS package (Didan 2015) in program R (v 3.6.1, R Core Team 2019) to download the data. Moose GPS-locations were overlaid on the EVI raster that temporally corresponded with the field data collection.

Moose Detection Modeling

After our first season in 2018, we used effect plots to visualize the relationship between the variables and adult moose detection (Table 1). We were specifically looking for what conditions influenced detection so we could improve our success during the 2019 season. The graphs indicated that decreased temperature and canopy cover, and greater cloud cover all increased detection. When modeling the 2018 data, we did not investigate the influence of EVI. We have provided an example of the effects of cloud cover from flights over a captive bison (Bison bison) herd located at the University of Minnesota's Cedar Creek Ecosystem Science Reserve where we tested our UAS and FLIR sensors prior to conducting surveys of wild moose (Fig. 2). Thermal survey flights during clear sky conditions resulted in unclear bison detections (Fig. 2A) relative to overcast sky conditions (Fig. 2B). During our second field season, we maximized detectability of moose by conducting flights earlier in the season (starting 25 April instead of 23 May), earlier in the morning (when ground temperature was at its lowest), and on days with greater cloud cover.

We hypothesized that canopy cover would have a strong influence on our ability to detect moose with our FLIR

Table 1. Detection model covariate names and descriptions with units, mean and SE, and ranges in observations, combined from 2018 and 2019 flight data from northeastern Minnesota, USA.

Variable	Definition	Units	Mean (SE)	Range
Altitude	Mean altitude of the UAV (m above ground)	Meters above ground	106.6 (1.20)	82.3–132.6
MooseDetect	Whether adult moose was detected or not (response variable)	Binary (0 = no, 1 = yes)	0.57 (0.05)	0–1
Canopy	Max. proportion of the canopy >3 m with 20-m buffer of the moose	Proportion	0.50 (0.02)	0.05–0.76
Cloud	Whether cloud cover was considered overcast or not	Binary (0 = no, 1 = yes)	0.16 (0.04)	0–1
Conifer	Proportion of the landcover in a 20-m buffer around the moose that was conifer or mixed forest	Proportion	0.25 (0.04)	0–1
EVI	Enhanced vegetation index—remotely sensed metric of vegetative greenness	Index (possible range: −2000–10000)	4210 (157.4)	2145.0–6843.0
Humid	Relative humidity recorded at nearest airport	Proportion	49.76 (1.71)	19.0–87.0
LaunchTime	UAV launch time (hours and minutes)	Hours	9:35 (00:20)	4:00–17:00
Temp	Temperature	°C	13.52 (0.74)	−1.11–27.22
Wind	Wind speed recorded at the nearest airport	Knots	5.42 (0.29)	0.00–11.3
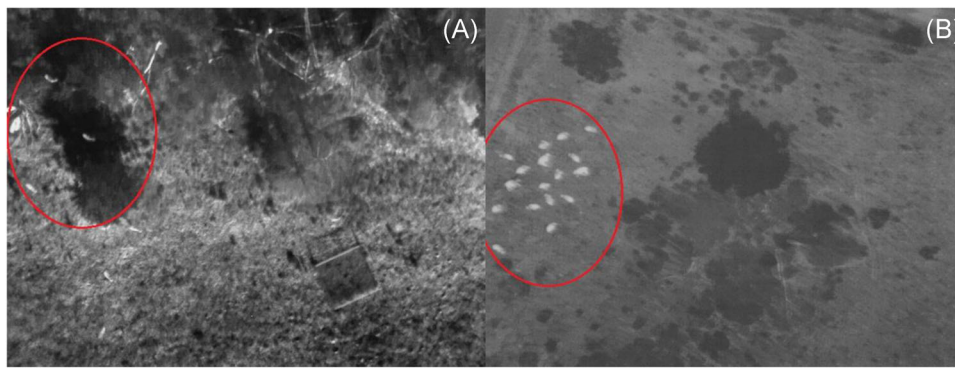
Figure 2. Side-by-side comparison of thermal infrared photos of a captive bison herd captured during clear sky conditions (A) and overcast sky conditions (B). Imagery was collected at the University of Minnesota's Cedar Creek Ecosystem Science Reserve, USA, during July 2018. This contrast demonstrates the positive effect that overcast sky conditions have on thermal detection.

sensor, so we created a set of univariate models in which we regressed different spatial extents of both the mean and maximum canopy cover around a given moose's GPS-location during the time of flight with our detection response. Each linear model contained one value for the scaled mean or maximum canopy cover at buffers of 20 m, 25 m, 30 m, 50 m, and 100 m. We used a generalized linear model structure with a binomial distribution in the glm function of program R and assessed the fit of each model using Akaike's Information Criteria adjusted for small sample sizes (AIC_c). The 20-m buffer with the maximum value for canopy cover explained the most deviance in moose detection so we used it in the full model of moose detection (see below) and used a 20-m buffer to create the total percentage of conifer and mixed conifer-deciduous forest.

To formally model moose detection (binary response: 0 = present but not detected, 1 = present and detected) for our combined two spring field seasons, we developed a set of 15 *a priori* models and a null model (intercept only). We restricted the total number of model parameters to 3 such that each model either contained 3 additive covariates or an interaction with additive effects for the 2 associated variables. We used the same generalized linear model structure described above for the canopy-cover buffer analysis. Within each model, all independent variables were centered and scaled by their corresponding standard deviation to improve model convergence, and we assessed relative model fit using AIC_c. Prior to fitting the models, we removed 3 observations due to covariate completeness (n = 89 flights).

We determined the strength of influence for each covariate in the top model(s) by creating effect plots using the package ggeffects (Lüdecke 2018) in program R. Each plot illustrates the mean and 95% confidence interval of predicted moose detection at each value of the covariate while all other variables are held constant at their mean values. We predicted moose detection across the 2.5% to the 97.5% quantile values to assess the change within the 95% distribution of the values we collected for the given covariate. All covariates used in the effect plots were created at their original scale (not centered and scaled) to better illustrate the relationships with familiar values (e.g., % of canopy cover, degrees Celsius).

Post Hoc Modeling

We collected sky condition observations from the same weather station that we used for our other weather-based covariates. We created an additional covariate using the National Oceanic and Atmospheric Administration's (NOAA 2019) cloud coverage classification to compare against our original field-based observation data of cloud cover (Cloud). The weather station-based covariate was binary with the NOAA classification for overcast coded as a 1 while all other observations, including missing, were coded as 0. To determine the relative importance of field vs weather-station derived cloud cover, we fit models with the centered and scaled values for Cloud (field-based) and compared the AIC_c and coefficient estimates to those from models based on the weather station estimates of cloud cover (n = 89 flights). We then removed all observations that corresponded to the weather station-based covariate's classification of missing and repeated the comparison (n = 82 flights). When comparing the detection percentages between field and weather station-based sky conditions, we had more flights with weather station-based data because some flights had missing field-based observations.

RESULTS

We conducted 92 total thermal UAS flights over cow moose from 2018 to 2019. Combined detection success over 2018 and 2019 was 57%; however, modifications to flight timing and procedures increased detection success from 25% in 2018 to 85% in 2019. Over the 2 years of our study we detected 18 individual cows, with multiple detections per cow. We had a combined calf detection success of 54% over the 2 study periods, confirming the detection of 18 individual calves. Similar to adult moose, calf detection improved from 27% in 2018 to 79% in 2019 after making adjustments to the timing of flights. During 2019, we confirmed 3 separate suspected predation events of calves with UAS thermal survey flights and disproved one that was
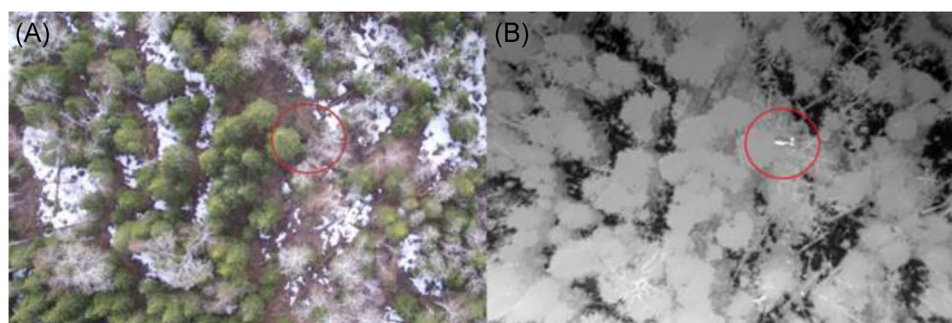
Figure 3. Comparison of UAS-gathered RGB imagery (A) and thermal infrared imagery (B) of a cow moose with two calves in northeastern Minnesota, USA, during spring of 2019. The photos were captured at the same time and location over this cow and her calves, which demonstrates the advantage of increased detection success from thermal infrared technology over RGB photography.

thought to be a successful predation. Only 46% of thermally detected moose in 2019 could be seen in corresponding RGB footage upon visual inspection. Vegetation and dark-colored terrain often obscured moose in RGB footage, whereas FLIR footage allowed for easy detection (Fig. 3).

Detection Analysis

Our top model of adult moose detection included the additive influences of vegetative greenness (EVI; $\widehat{\beta} = -1.37$, SE = 0.32), whether cloud cover was considered overcast or not (Cloud; $\widehat{\beta} = 1.13$, SE = 0.43), and maximum canopy cover (Canopy; $\widehat{\beta} = -1.10$, SE = 0.38; scaled and centered; Table 2, Fig. 4). From the lowest to the highest values of the 95% distribution of observed EVI values (Fig. 4A), our top-fitting model predicted moose detection would decrease from 92.6% (95% CI = 80.7%–97.4%; EVI = 2160) to 18.0% (95% CI = 6.4%–41.3%; EVI = 6512). Detectability increased during flights with overcast skies ($\overline{X}$ = 96.2%, 95% CI = 73.2%–99.6%) relative to flights occurring during conditions without overcast skies ($\overline{X}$ = 53.7%, 95% CI = 38.3%–68.5%; Fig. 4B). Moose detection also decreased with more canopy cover around the moose's

location (20 m buffer) from a prediction of 96.4% (95% CI = 77.2%–99.5%; Canopy = 13.1%) to 29.9% (95% CI = 13.3%–54.2%; Canopy = 70.7%; Fig. 4C). Temperature was not included in the top model; however, it did exhibit a somewhat strong negative effect on moose detection (Temp; $\widehat{\beta} = -0.90$, SE = 0.37).

Post Hoc Analysis of Cloud Cover

Weather station-based observations of cloud cover did not explain as much variation in moose detection as field-based observations of cloud cover. Our field-based assessment of overcast (Cloud = 1) was associated with 13 moose detections and only one non-detection (92.9% [13/14]). In comparison, the weather station-based classification of overcast was associated with a positive detection during 16, and a non-detection during 4, flights (80% [16/20]). When our best-supported model (n = 89 flights) included weather station-based data where missing data were considered not to be overcast (coded as 0), AIC_c increased by 7.28; the scaled and centered coefficient value ($\widehat{\beta} = 0.58$, SE = 0.30) was smaller than our original covariate estimate for Cloud ($\widehat{\beta} = 1.13$, SE = 0.43). Models where all missing values in

Table 2. All 16 models considered when assessing the factors influencing the detection (binary) of adult moose in northeastern Minnesota, USA, using UAS with thermal sensors during the spring of 2018 and 2019. We used generalized linear models with a binomial distribution and restricted the number of parameters to a maximum of three.

Model	logLik	ΔAIC_c	Weight
EVI + Cloud + Canopy	−35.55	0.00	0.86
Canopy + EVI + Temp	−37.66	4.24	0.10
Cloud + EVI + Temp	−39.16	7.22	0.02
Canopy + EVI + Canopy × EVI	−40.05	9.02	0.01
Cloud + Temp + Cloud × Temp	−42.17	13.25	0.00
Conifer + Cloud + Temp	−42.64	14.19	0.00
Altitude + LaunchTime + Temp	−42.82	14.56	0.00
EVI + Humid + Wind	−43.87	16.64	0.00
Altitude + Canopy + Altitude × Canopy	−44.73	18.37	0.00
Altitude + EVI + Altitde × EVI	−45.21	19.32	0.00
Altitude + Conifer + LaunchTime	−47.00	22.92	0.00
Canopy + Cloud + Humid	−47.33	23.57	0.00
Canopy + Conifer + Canopy × Conifer	−52.83	34.58	0.00
Cloud + Humid + Wind	−54.98	38.87	0.00
Humid + LaunchTime + Wind	−56.29	41.50	0.00
Intercept only (NULL)	−60.74	43.95	0.00
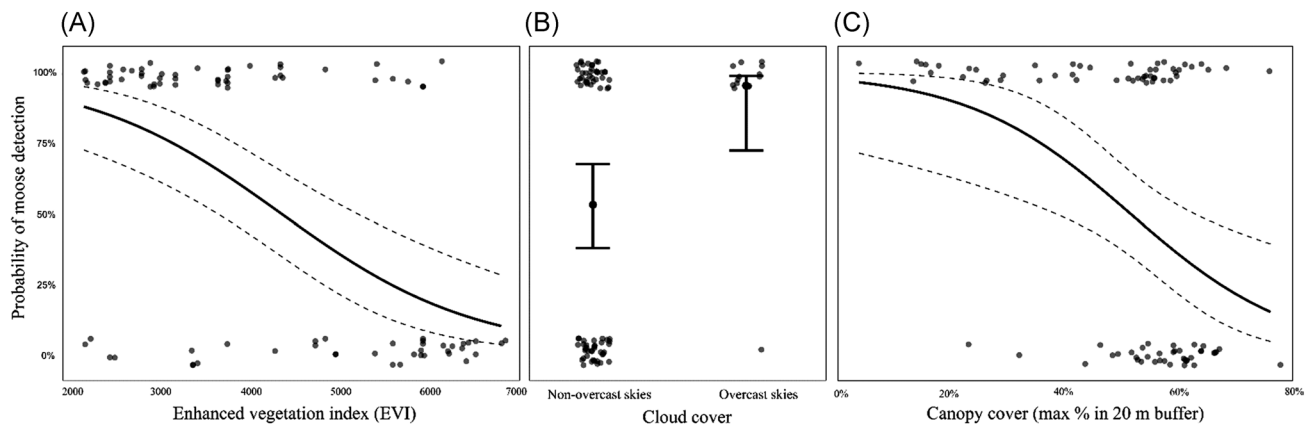
Figure 4. Detection success of GPS-collared adult cow moose in northeastern Minnesota, USA, during spring of 2018 and 2019 using thermal technology mounted on a UAS. Moose detections are plotted as raw values on the y-axis as either 100% (present and detected) or 0% (present but not detected). The predicted mean and 95% confidence intervals are based on the best-supported model for detection. We predicted moose detection for all sampled values of A) the remotely-sensed enhanced vegetation indices (EVI) over the moose's location, B) whether or not the sky was overcast during the flight (field-observation) while holding the other values in the best-supported model at their means, and C) maximum canopy cover around the moose's GPS location during the time of the flight.

the weather station-based data were removed (n = 82 flights) resulted in an increased AIC_c of 7.49 compared to the field-based observation cloud cover model; the covariate estimates were again smaller as well (weather station-based cloud cover: $\hat{\beta} = 0.61$, SE = 0.32; field observation cloud cover: $\hat{\beta} = 1.17$, SE = 0.44).

DISCUSSION

We successfully applied UAS technology and FLIR sensors to detect collared adult cow moose and calves in a heavily forested region of northeastern Minnesota. The increase in detection success from our first to our second field season was a result of developing preliminary relationships between adult moose detection and environmental and temporal covariates. This improvement provides validation that our final detection model (which incorporated both years of flight data) captured useful relationships for researchers planning to conduct ungulate surveys with UAS and FLIR technology. We maximized detection success during our second season by conducting survey flights earlier in the calving season to take advantage of leaf-free conditions. We also concentrated our flight efforts within the early morning hours when temperatures were coolest, and less thermal energy was being emitted from ground objects. Snow cover present in our second season (2019) during the early spring also improved thermal detection by covering ground objects and maximizing the thermal contrast between moose and their environment. Importantly, our research provides a valuable method for determining ungulate reproductive success and calf survival using a less invasive method than handling and collaring calves, which may induce additional stressors (Del Giudice et al. 2015).

Our FLIR-equipped UAS demonstrated clear advantages over conventional methodology for monitoring moose calving success by increasing animal detectability while reducing survey cost and effort. The inclusion of FLIR sensing with UAS was crucial for detecting cow-calf pairs in forested environments. Moose were often obscured by canopy cover in RGB footage, whereas FLIR footage allowed for easy detection (Fig. 3). Challenges of visual detection without FLIR are also reflected in the state-wide aerial counts conducted by the MNDNR. The MNDNR reported an average estimated detection probability of 61% for their 2018 aerial survey using conventional aircraft and visual observation (Del Giudice 2018), compared to our detection probability of 85% using UAS and FLIR technology. Further, unmanned aerial systems offered a relatively cheap method to collect aerial data (e.g., Vermeulen et al. 2013), and following the initial financial investment for UAS equipment our operating costs were minimal, with ground transportation being our largest field expenditure.

Integrating OBIA methods for detecting wildlife in aerial imagery is a promising approach that can accurately automate detection (Witharana and Lynch 2016, Chabot et al. 2018). Chrétien et al. (2016) applied OBIA to detect ungulates from UAS imagery and reported 100% detection rates in some surveys; this success was accomplished with very high-resolution sensors (Guirado et al. 2017). We employed an economical FLIR sensor with relatively low resolution (640 × 512), as is common for wildlife research (Witczuk et al. 2018), and experienced challenges using OBIA. Flying the UAS at lower altitudes may have compensated for low resolution but would have increased the potential to disturb moose and have been problematic for terrain avoidance. Dense forest further convoluted the OBIA process because of the many bright returns caused by heated, non-living ground objects among the trees. These objects sometimes resembled moose in brightness and shape (e.g., vegetation would distort the recognizable silhouette of a moose), greatly decreasing the ability of OBIA software to accurately classify objects. Instead, we opted to manually review the video footage, which served to be a simple and efficient way to identify collared moose, and was especially effective for identifying calves present with cows

(distinguishing different sized targets with OBIA adds further complexity). Manual detection required ~16 combined hours per observer over our two seasons, averaging ~10 min per UAS flight for each observer. Until sensors with higher resolution become more economical, or OBIA methods overcome lower resolution limitations, the technical hurdles of implementing OBIA may only be worthwhile for researchers with access to high-resolution sensors and those attempting to detect non-collared animals, especially over large spatial extents.

The accuracy of conventional methodology for monitoring reproduction (e.g., observing calf tracks) can also be questionable (Y. C. Ibrahim, Grand Portage Trust Lands, personal communication). The use of UAS and FLIR sensing enabled us to confirm suspected predation events with greater certainty. While GPS data from collared cows can show movements indicative of predation events, as described by Obermoller et al. (2019), relying solely on this method does not always reliably detect the fate of the calf. For example, after a cow in our study had demonstrated the indicative movements of a predation event, UAS thermal imagery revealed that the calf had survived and was still with the cow after the event. This suggests that repeated UAS flights over collared cows can provide a low-disturbance method to monitor calf survival during the first month of their lives, and again following leaf fall in autumn.

Unmanned aerial systems were less disruptive than typical approaches for monitoring calving success and calf survival. Capturing moose calves and fitting them with GPS or VHF collars is a popular method for examining calf survival (Ballard et al. 1981, Patterson et al. 2013, Severud et al. 2015); however, this approach has an inherent risk of capture-related mortality, with abandonment shown to be the leading cause of capture-induced calf mortality (Livezey 1990). Del Giudice et al. (2015) reported that 18.4% of captured neonate moose were abandoned within 48 hours post capture during an initial study of calf mortality in northeastern Minnesota. Phillips and Alldredge (2000) observed that continued human disturbance of elk from ground approaches during the peak calving season decreased calf-cow ratios in their study population, and it is conceivable that similar impacts may be experienced by moose. Our survey protocols were designed to minimize the chance of UAS-specific moose disturbance, and we gauged levels of disruption by monitoring animal behavior (derived from GPS-collar relocation data) following each flight. We identified one individual cow who made a >1 km movement beginning just 7 min after the UAS was launched. This rate of movement is not unusual for moose (E. Isaac, Grand Portage Trust Lands, personal communication); however, it did not occur with other moose during other flights. Because we approached this site on foot through dense vegetation (for other flights, we limited the noises of our approach by launching from a gravel road accessed by vehicle or from a walking trail), it is possible that our approach, rather than the UAS, ultimately caused the cow to flee the area.

We considered a lack of behavioral response by moose to be evidence of no disturbance from UAS flights, similar to Vermeulen et al. (2013), and Goebel et al. (2015) in their UAS studies of elephants and penguins (*Pygoscelis spp.*), respectively. It is important to keep in mind, however, that disturbance may cause unseen physiological stress in wildlife that do not exhibit any overt behavioral response (Ditmer et al. 2015). Although animals may acclimate to repeated low-altitude UAS flights (Ditmer et al., 2019), we echo the UAS ethical guidelines outlined by Hodgson and Koh (2016) regarding wildlife disturbance: flights should be conducted no lower in altitude than is necessary for data collection and repeat flights over individuals should only be done when it is necessary to collect critical data.

One major challenge of conducting wildlife surveys with FLIR-technology is that solar energy can reduce detection by complicating the identification of target animals. Solar radiation heats the ground and non-target objects (e.g., rocks, stumps, trees), which in turn create noise, or thermal bright spots in an image, leading to potential false-positive detections or masking of target animals (Dunn et al. 2002, Chrétien et al. 2016, Lethbridge et al. 2019). Similar to Millette et al. (2011), who conducted thermal surveys of moose from a manned aircraft, our results for cloud cover and temperature on moose detection demonstrated this phenomenon. Increased cloud cover improved thermal detection probability because clouds blocked some amount of solar energy from reaching objects on the ground, thus maximizing the thermal contrast between moose and their surroundings and reducing the potential for misidentifying a non-moose object as a moose. Localized changes in cloud cover and the resulting thermal heating of ground objects were illustrated by our findings that field-based cloud cover observations explained more variation in detection in our model than weather station-based observations. For example, during preliminary testing of our UAS, thermal imagery collected on different days (clear vs. overcast), but at the same time of day and with similar ambient temperatures (20.0°C and 16.1°C), dramatically altered our ability to visually count the known number of individual bison present (see Fig. 2).

Remotely-sensed data describing forest canopy cover and phenological measures of greenness, such as NDVI or EVI, can greatly enhance UAS operators' understanding of where and when to conduct flights to maximize efficiency in forested environments. Although coniferous cover has been repeatedly shown to limit thermal detection of animals (Garner et al. 1995, Dunn et al. 2002, Potvin and Breton 2005), the impacts of deciduous canopy phenology are less well known. As expected, we found that canopy cover and EVI negatively influenced detection success, since greater closure of deciduous tree canopy and denser green vegetation can block the thermal energy of moose from reaching our FLIR sensor. This was supported by our observation of declining detection success in 2019 as the deciduous tree canopy progressed from leafless towards full leaf-out. Indeed, even when we could detect moose that were partially obscured by vegetation, their thermal image

appeared distorted in both shape and intensity of the heat signature, a phenomenon also reported by Wiggers and Beckerman (1993). Although FLIR technology greatly enhanced our ability to detect moose relative to RGB alone, we still failed to detect moose that were completely obscured by deciduous tree canopy or located within very dense conifer stands.

A limitation to using NASA's MODIS products to assist in planning surveys is the time lag between the median date of the 16-day composite EVI data and when it becomes publicly available (~1 month based on our recent downloads). Using greenness indices from previous years could allow for identifying areas with less vegetative cover (increased detection), but the current lag in data availability is a significant hurdle to successfully incorporating this product into surveys of the same year. Winter and leafless periods of fall and spring clearly yield the greatest potential for successful FLIR detection. The increase in detection success during our second field season was certainly a direct result of our efforts to fly prior to deciduous leaf-out. It is important to remember that our study occurred in a boreal ecosystem near 48° N latitude. Thus, the strong relationships we found in our detection models may only be valid in forested environments and where temperature differentials between target species and ambient temperatures are relatively large (i.e., temperate or cooler environments). When possible, we recommend that researchers conduct test flights with captive animals before initiating extensive studies, to familiarize themselves with the way local vegetation types and structure may hinder detection during field research.

Despite the clear benefits of UAS for wildlife surveys, current regulations still reduce operational efficiency. Although much has improved in the last five years regarding ease of compliance with federal regulations, many of the regulatory hurdles outlined by Vincent et al. (2015) still stand. Most importantly, regulations prohibiting operation beyond visual line of sight (BVLOS) or at night severely limited our ability to efficiently target animals. The BVLOS requirement, which requires the operator to maintain unaided visual contact with the UAS at all times of the flight, was especially burdensome in our forested study area. Likewise, we were prohibited from surveying during the night and early morning before dawn—times when the thermal contrast between wildlife and the ground, as well as other non-living objects, are at their greatest (Mulero-Pázmány et al. 2014, Witczuk et al. 2018). Indeed, Ireland et al. (2019) concluded that conducting white-tailed deer surveys with FLIR-equipped UAS was optimized at night because of maximized thermal contrast. The Federal Aviation Administration can grant waivers to relax some flight restrictions, but approvals are not guaranteed, and the application process can be lengthy and often unrealistic for the temporal demands of field seasons.

Hardware limitations of UAS impact their effectiveness and ease of use for inexperienced UAS pilots and crew. Short battery endurance, as was outlined by Linchant et al. (2015), is one such limitation. Our maximum flight endurance with our payload configuration was ~20 min, which reduced our survey size and maximum distance the UAS could travel from launch points when visual contact was not an issue. Endurance limitations were not insurmountable for calf monitoring of GPS-collared moose; however, short flight endurance combined with BVLOS restrictions currently limit the potential for UAS to be applied to large-scale population monitoring over extensive forested areas. Manned aircraft still excel in such situations due to greater autonomy.

Weather conditions impacted our ability to operate and successfully detect animals. Precipitation prevented flight operations because of the potential for water damage to equipment (Duffy et al. 2017) and the negative effect on thermal image quality. Burke et al. (2018) described how condensed airborne water droplets, such as fog, will decrease data quality of FLIR imagery due to water vapor readily absorbing longwave radiation (Gordon et al. 2007). Our results from test flights in foggy conditions corroborated this. Heavy winds can impact flight stability and be hazardous for UAS operations in close proximity to trees, thus Weissensteiner et al. (2015) recommended that operations in forested environments only be conducted during calm wind conditions. Flight turbulence also decreased the quality of our thermal data by creating blurred imagery and shaky video footage. Winds greater than 35 km/hr during our study were rare, but these conditions and other inclement weather grounded our flight operations for safety and data quality for ~16% of our attempted field days.

Our reliance on a weather reporting station ~215 km from our flight operations was done to standardize our weather data and was the nearest and most comparable source of historic weather data. However, we recommend a field-based weather meter for future operations to collect measurements at specific flight locations. Field-based meters collect real-time weather conditions, which should be more robust for detection modeling and flight planning than weather station-based data. Findings from our post hoc analysis demonstrated that weather station-based cloud cover data explained less variation in moose detection than our field-based observations due to localized variation in cloud cover. We hypothesized that temperature and relative humidity, which were also collected from the weather station, would be significantly associated with moose detection. However, neither were in our top model; again, potentially due to the different conditions experienced at the flight location versus the weather station.

Our work served to hone UAS methodology for the application of wildlife research. We found that a readily available off-the-shelf UAS equipped with FLIR technology was an effective platform for detecting collared moose and counting and monitoring calves in a densely forested environment. We identified several ongoing environmental challenges and technical limitations, but we also realized significant improvement in detection success from one season to the next. Our efforts to model factors driving moose detectability allowed us to establish best practices for maximizing UAS efficacy with FLIR sensing for surveys of forest-dwelling animals. It is likely that the continued

improvement and reduced costs of UAS (Baxter and Hamilton 2018), and associated sensors, will open new doors to the types of data collection possible and expand on potential target species. We postulate that FLIR sensor-equipped UAS—especially with the capability to collect geo-tagged thermal imagery—could be effective for monitoring reproductive success (e.g., birthing success, twinning rate, and young survival) of other GPS-collared, large-bodied mammals.

ACKNOWLEDGMENTS

LITERATURE CITED

Adams, K. P., P. J. Pekins, K. A. Gustafson, and K. Bontaites. 1997. Evaluation of infrared technology for aerial moose surveys in New Hampshire. Alces 33:129–139.

Addison, R. B. 1972. The possible use of thermal infrared imagery for wildlife census. Proceedings of the 8th North American Moose Conference and Workshop 8:301–325.

Anderson, K., and K. J. Gaston. 2013. Lightweight unmanned aerial vehicles will revolutionize spatial ecology. Frontiers in Ecology and the Environment 11:138–146.

Ballard, W. B., T. H. Spraker, and K. P. Taylor. 1981. Causes of neonatal moose calf mortality in south central Alaska. Journal of Wildlife Management 45:335–342.

Baxter, P. W. J., and G. Hamilton. 2018. Learning to fly: integrating spatial ecology with unmanned aerial vehicle surveys. Ecosphere 9.

Beaver, J. T., R. W. Baldwin, M. Messinger, C. H. Newbolt, S. S. Ditchkoff, and M. R. Silman. 2020. Evaluating the use of drones equipped with thermal sensors as an effective method for estimating wildlife. Wildlife Society Bulletin 44:434–443.

Bennitt, E., H. L. A. Bartlam-Brooks, T. Y. Hubel, and A. M. Wilson. 2019. Terrestrial mammalian wildlife responses to Unmanned Aerial Systems approaches. Scientific Reports 9:2142.

Bernatas, S., and L. Nelson. 2004. Sightability model for California bighorn sheep in canyonlands using forward-looking infrared (FLIR). Wildlife Society Bulletin 32:638–647.

Bontaites, K. M., K. A. Gustafson, and R. Makin. 2000. A Gasaway-type moose survey in New Hampshire using infrared thermal imagery: preliminary results. Alces 36:69–75.

Burke, C., M. Rashman, S. Wich, A. Symons, C. Theron, and S. Longmore. 2018. Optimising observing strategies for monitoring animals using drone-mounted thermal infrared cameras. International Journal of Remote Sensing 40:439–467.

Carstensen, M., E. C. Hildebrand, D. Plattner, M. Dexter, V. St-Louis, C. Jennelle, and R. G. Wright. 2017. Determining cause-specific mortality of adult moose in northeast Minnesota, February 2013–July 2016. Minnesota Department of Natural Resources, Wildlife Health Program. Forest Lake, Minnesota, USA.

Chabot, D. 2009. Systematic evaluation of a stock unmanned aerial vehicle (UAV) system for small-scale wildlife survey applications. Thesis, McGill University, Montreal, Québec, Canada.

Chabot, D., and D. M. Bird. 2012. Evaluation of an off-the-shelf unmanned aircraft system for surveying flocks of geese. Waterbirds 35:170–174.

Chabot, D., C. Dillon, and C. M. Francis. 2018. An approach for using off-the-shelf object-based image analysis software to detect and count birds in large volumes of aerial imagery. Avian Conservation and Ecology 13:15.

Chen, S., G. J. McDermid, G. Castilla, and J. Linke. 2017. Measuring vegetation height in linear disturbances in the boreal forest with UAV photogrammetry. Remote Sensing 9:1257.

Chrétien, L., J. Théau, and P. Ménard. 2015. Wildlife multispecies remote sensing using visible and thermal infrared imagery acquired from an unmanned aerial vehicle (UAV). International Archives of the Photogrammetry, Remote Sensing and Spatial Information Sciences XL-1/W4:241–248.

Chrétien, L. -P., J. Théau, and P. Ménard. 2016. Visible and thermal infrared remote sensing for the detection of white-tailed deer using an unmanned aerial system. Wildlife Society Bulletin 40:181–191.

Del Giudice, G. D. 2018. 2018 Aerial moose survey. Minnesota Department of Natural Resources, Forest Wildlife Populations and Research Group. Grand Rapids, Minnesota, USA.

Del Giudice, G. D., W. J. Severud, T. R. Obermoller, R. G. Wright, T. A. Enright, and V. St-Louis. 2015. Monitoring movement behavior enhances recognition and understanding of capture-induced abandonment of moose neonates. Journal of Mammalogy 96:1005–1016.

Didan, K. 2015. MOD13A2 MODIS/Terra vegetation indices 16-Day L3 global 1km SIN grid V006 [Data set]. NASA EOSDIS Land Processes DAAC. <https://doi.org/10.5067/MODIS/MOD13A2.006>. Accessed 3 Jan 2021.

Ditmer, M. A., J. B. Vincent, L. K. Werden, J. C. Tanner, T. G. Laske, P. A. Iaizzo, D. L. Garshelis, and J. R. Fieberg. 2015. Bears show a physiological but limited behavioral response to unmanned aerial vehicles. Current Biology 25:2278–2283.

Ditmer, M. A., L. K. Werden, J. C. Tanner, J. B. Vincent, P. Callahan, P. A. Iaizzo, T. G. Laske, and D. L. Garshelis. 2019. Bears habituate to the repeated exposure of a novel stimulus, unmanned aircraft systems. Conservation Physiology 7:1–7.

Duffy, J. P., A. M. Cunliffe, L. Debell, C. Sandbrook, S. A. Wich, J. D. Shutler, I. H. Myers-smith, M. R. Varela, and K. Anderson. 2017. Location, location, location: considerations when using lightweight drones in challenging environments. Remote Sensing in Ecology and Conservation 4:7–19.

Dunn, W. C., J. P. Donnelly, and W. J. Krausmann. 2002. Using thermal infrared sensing to count elk in the southwestern United States. Wildlife Society Bulletin 30:963–967.

Ezat, M. A., C. J. Fritsch, and C. T. Downs. 2018. Use of an unmanned aerial vehicle (drone) to survey Nile crocodile populations: a case study at Lake Nyamithi, Ndumo Game Reserve, South Africa. Biological Conservation 223:76–81.

Focardi, S., A. M. De Marinis, M. Rizzotto, and A. Pucci. 2001. Comparative evaluation of thermal infrared imaging and spotlighting to survey wildlife. Wildlife Society Bulletin 29:133–139.

Garner, D. L., H. B. Underwood, and W. F. Porter. 1995. Use of modern infrared thermography for wildlife population surveys. Environmental Management 19:233–238.

Gill, R. M. A., M. L. Thomas, and D. Stocker. 1997. The use of portable thermal imaging for estimating deer population density in forest habitats. Journal of Applied Ecology 34:1273–1286.

Goebel, M. E., W. L. Perryman, J. T. Hinke, D. J. Krause, N. A. Hann, S. Gardner, and D. J. LeRoi. 2015. A small unmanned aerial system for estimating abundance and size of Antarctic predators. Polar Biology 38:619–630.

Gordon, I. E., L. S. Rothman, R. R. Gamache, D. Jacquemart, C. Boone, P. F. Bernath, M. W. Shephard, J. S. Delamere, and S. A. Clough. 2007. Current updates of the water-vapor line list in HITRAN: a new diet for

air-broadened half-widths. Journal of Quantitative Spectroscopy and Radiative Transfer 108:389–402.

Guirado, E., S. Tabik, D. Alcaraz-Segura, J. Cabello, and F. Herrera. 2017. Deep-learning versus OBIA for scattered shrub detection with Google Earth imagery: ziziphus lotus as case study. Remote Sensing 9:1220.

Haroldson, B. S., E. P. Wiggers, J. Beringer, L. P. Hansen, and J. B. McAninch. 2003. Evaluation of aerial thermal imaging for detecting white-tailed deer in a deciduous forest environment. Wildlife Society Bulletin 31:1188–1197.

Hodgson, A., N. Kelly, and D. Peel. 2013. Unmanned aerial vehicles (UAVs) for surveying marine fauna: a dugong case study. PLoS ONE 8:1–15.

Hodgson, J. C., and L. P. Koh. 2016. Best practice for minimising unmanned aerial vehicle disturbance to wildlife in biological field research. Current Biology 26:R404–R405.

Hodgson, J. C., R. Mott, S. M. Baylis, T. T. Pham, S. Wotherspoon, A. D. Kilpatrick, R. Raja Segaran, I. Reid, A. Terauds, and L. P. Koh. 2018. Drones count wildlife more accurately and precisely than humans. Methods in Ecology and Evolution 2018:1–8.

Ireland, A. W., D. A. Palandro, V. Y. Garas, R. W. Woods, R. A. Davi, J. D. Butler, D. M. Gibbens, and J. S. Gibbens. 2019. Testing unmanned aerial systems for monitoring wildlife at night. Wildlife Society Bulletin 43:182–190.

Israel, M. 2011. A UAV-based roe deer fawn detection system. International Archives of the Photogrammetry, Remote Sensing and Spatial. Information Sciences 38:51–55.

Jiménez López, J., and M. Mulero-Pázmány. 2019. Drones for conservation in protected areas: present and future. Drones 3:1–23.

Jones, G. P. IV, L. G., Pearlstine, and H. F. Percival. 2006. An assessment of small unmanned aerial vehicles for wildlife research. Wildlife Society Bulletin 34:750–758.

Kissell, R. E., and S. K. Nimmo. 2011. A technique to estimate white-tailed deer (Odocoileus virginianus) density using vertical-looking infrared imagery. Wildlife Biology 17:85–92.

Kiszka, J. J., J. Mourier, K. Gastrich, and M. R. Heithaus. 2016. Using unmanned aerial vehicles (UAVs) to investigate shark and ray densities in a shallow coral lagoon. Marine Ecology Progress Series 560:237–242.

Lethbridge, M., M. Stead, and C. Wells. 2019. Estimating kangaroo density by aerial survey: a comparison of thermal cameras with human observers. Wildlife Research 46:639–648.

Lhoest, S., J. Linchant, S. Quevauvillers, C. Vermeulen, and P. Lejeune. 2015. How many hippos: algorithm for automatic counts of animals with infra-red thermal imagery from UAV. International Archives of the Photogrammetry, Remote Sensing and Spatial Information Sciences 40:355–362.

Linchant, J., G. A. Tech, and F. R. Management. 2015. Are unmanned aircraft systems (UASs) the future of wildlife monitoring? A review of accomplishments and challenges. Mammal Review 45:239–252.

Livezey, K. B. 1990. Toward the reduction of marking-induced abandonment of newborn ungulates. Wildlife Society Bulletin 18:193–203.

Lüdecke, D. 2018. ggeffects: Tidy data frames of marginal effects from regression models. Journal of Open Source Software 3:772.

Marsh, H., and D. F. Sinclair. 1989. Correcting for visibility bias in strip transect aerial surveys of aquatic fauna. Journal of Wildlife Management 53:1017–1024.

Millette, T. L., E. Marcano, and D. Laflower. 2014. Winter distribution of moose at landscape scale in northeastern Vermont: a GIS analysis. Alces 50:17–26.

Millette, T. L., D. Slaymaker, E. Marcano, C. Alexander, and L. Richardson. 2011. Aims-thermal—a thermal and high resolution color camera system integrated with GIS for aerial moose and deer census in northeastern Vermont. Alces 47:27–37.

Minnesota Geospatial Information Office. 2016. Minnesota land cover classification and impervious surface area by landsat and lidar: 2013 update—version 2. https://gisdata.mn.gov/dataset/base-landcover-minnesota>. Accessed 20 Nov 2019.

Minnesota Geospatial Information Office. 2018. Phase 3—Arrowhead Region data. <http://www.mngeo.state.mn.us/committee/elevation/mn_elev_mapping.html>. Accessed 20 Nov 2019.

Montague, D. M., R. D. Montague, M. L. Fies, and M. J. Kelly. 2017. Using distance-sampling to estimate density of white-tailed deer in

forested, mountainous landscapes in Virginia. Northeast Naturalist 24:505–519.

Mulero-Pázmány, M., S. Jenni-Eiermann, N. Strebel, T. Sattler, J. J. Negro, and Z. Tablado. 2017. Unmanned aircraft systems as a new source of disturbance for wildlife: a systematic review. PLoS ONE 12:1–14.

Mulero-Pázmány, M., R. Stolper, L. D. Van Essen, J. J. Negro, and T. Sassen. 2014. Remotely piloted aircraft systems as a rhinoceros anti-poaching tool in Africa. PLoS One 9:1–10.

National Oceanic and Atmospheric Administration [NOAA]. 2019. Climate data online. Local climatological data station details for Cook Municipal Airport, MN, USA. <https://www.ncdc.noaa.gov/data-access>. Accessed 27 Sep 2019.

Obermoller, T. R., G. D. Delgiudice, and W. J. Severud. 2019. Maternal behavior indicates survival and cause-specific mortality of moose calves. Journal of Wildlife Management 00:1–11.

Olsoy, P. J., L. A. Shipley, J. L. Rachlow, J. S. Forbey, N. F. Glenn, M. A. Burgess, and D. H. Thornton. 2018. Unmanned aerial systems measure structural habitat features for wildlife across multiple scales. Methods in Ecology and Evolution 9:594–604.

Patterson, B. R., J. F. Benson, K. R. Middel, K. J. Mills, A. Silver, and M. E. Obbard. 2013. Moose calf mortality in central Ontario, Canada. Journal of Wildlife Management 77:832–841.

Phillips, G. E., and A. W. Alldredge. 2000. Reproductive success of elk following disturbance by humans during calving season. Journal of Wildlife Management 64:521–530.

Potvin, F., and L. Breton. 2005. Testing 2 aerial survey techniques on deer in fenced enclosures—visual double-counts and thermal infrared sensing. Wildlife Society Bulletin 33:317–325.

R Core Team. 2019. R: a language and environment for statistical computing. R Foundation for Statistical Computing, Vienna, Austria. https://www.R-project.org/

Sardá-Palomera, F., G. Bota, C. Viñolo, O. Pallarés, V. Sazatornil, L. Brotons, S. Gomáriz, and F. Sardá. 2012. Fine-scale bird monitoring from light unmanned aircraft systems. Ibis 154:177–183.

Sasse, D. B. 2003. Job-related mortality of wildlife workers in the United States, 1937-2000. Wildlife Society Bulletin 31:1015–1020.

Severud, W. J., G. Del Giudice, T. R. Obermoller, T. A. Enright, R. G. Wright, and J. D. Forester. 2015. Using GPS collars to determine parturition and cause-specific mortality of moose calves. Wildlife Society Bulletin 39:616–625.

Severud, W. J., T. R. Obermoller, G. D. Delgiudice, and J. R. Fieberg. 2019. Survival and cause-specific mortality of moose calves in northeastern Minnesota. Journal of Wildlife Management 83(5):1131–1142.

Street, G. M., J. Fieberg, A. R. Rodgers, M. Carstensen, R. Moen, S. A. Moore, S. K. Windels, and J. D. Forester. 2016. Habitat functional response mitigates reduced foraging opportunity: implications for animal fitness and space use. Landscape Ecology 31:1939–1953.

van Andel, A. C., S. A. Wich, C. Boesch, L. P. Koh, M. M. Robbins, J. Kelly, and H. S. Kuehl. 2015. Locating chimpanzee nests and identifying fruiting trees with an unmanned aerial vehicle. American Journal of Primatology 77:1122–1134.

Verma, S. K., M. Carstensen, R. Calero-Bernal, S. A. Moore, T. Jiang, C. Su, and J. P. Dubey. 2016. Seroprevalence, isolation, first genetic characterization of Toxoplasma gondii, and possible congenital transmission in wild moose from Minnesota, USA. Parasitology Research 115:687–690.

Vermeulen, C., P. Lejeune, J. Lisein, P. Sawadogo, and P. Bouché. 2013. Unmanned aerial survey of elephants. PLoS One 8:e54700.

Vincent, J. B., L. K. Werden, and M. A. Ditmer. 2015. Barriers to adding UAVs to the ecologist's toolbox. Ecological Society of America 13:74–75.

Watts, A. C., J. H. Perry, S. E. Smith, M. A. Burgess, B. E. Wilkinson, Z. Szantoi, P. G. Ifju, and H. F. Percival. 2010. Small unmanned aircraft systems for low-altitude aerial surveys. Journal of Wildlife Management 74:1614–1619.

Weiskopf, S. R., O. E. Ledee, and L. M. Thompson. 2019. Climate change effects on deer and moose in the midwest. Journal of Wildlife Management 83:769–781.

Weissensteiner, M. H., J. W. Poelstra, and J. B. W. Wolf. 2015. Low-budget ready-to-fly unmanned aerial vehicles: an effective tool for

evaluating the nesting status of canopy-breeding bird species. Journal of Avian Biology 46:425–430.

Wiggers, E. P., and S. E. Beckerman. 1993. Use of thermal infrared sensing to survey white-tailed deer populations. Wildlife Society Bulletin 21:263–268.

Witczuk, J., S. Pagacz, A. Zmarz, and M. Cypel. 2018. Exploring the feasibility of unmanned aerial vehicles and thermal imaging for ungulate surveys in forests—preliminary results. International Journal of Remote Sensing 39:5504–5521.

Witharana, C., and H. J. Lynch. 2016. An object-based image analysis approach for detecting penguin guano in very high spatial resolution satellite images. Remote Sensing 8:375.

Wünschmann, A., A. G. Armien, E. Butler, M. Schrage, B. Stromberg, J. B. Bender, A. M. Firshman, and M. Carstensen. 2015. Necropsy findings in 62 opportunistically collected free-ranging moose (*Alces alces*) from Minnesota, USA (2003–13). Journal of Wildlife Diseases 51:157–165.

Associate Editor: Rodgers.